

# Mercaptopropyl Functionalized Polymethylsilsesquioxane Microspheres Prepared by Co-Condensation Method as Organosilica-Based Chromatographic Packings

Jiali Li<sup>1</sup> · Zhixia Huo<sup>1</sup> · Lei Chen<sup>1</sup> · Qian-Hong Wan<sup>1</sup> 

Received: 24 March 2017 / Revised: 25 June 2017 / Accepted: 30 June 2017 / Published online: 13 July 2017  
© Springer-Verlag GmbH Germany 2017

**Abstract** Mercaptopropyl functionalized polymethylsilsesquioxane microspheres have been prepared by a two-step acid/base catalyzed hydrolysis and co-condensation of methyltrimethoxysilane (MTMS) and mercaptopropyltrimethoxysilane (MpTMS) precursors. The mercaptopropyl loading of the microspheres is controlled by regulating the ratio of MpTMS to MTMS in the reaction feedstock. A pronounced decrease in surface area, pore volume, and pore size with increasing mercaptopropyl loading was observed and a transition in pore structure from mesopores to micropores/nearly nonporous occurred at mole fractions of mercaptopropyl groups greater than 0.23. The resulting particles exhibited low silanol/thiol activity as both the concentrations and dissociation constants of the acidic groups were considerably lower than those reported for inorganic silica-based packings. Chromatographic evaluation using a test mixture containing uracil, toluene, ethylbenzene, quinizarin, and amitriptyline revealed that the new materials possess typical reverse phase chromatographic properties with moderate methylene selectivity and intrinsic inertness to bases. Taken together, the mercaptopropyl functionalized microspheres are a promising alternative to base-deactivated silica-based packings for the separation of the basic compounds which constitute a large proportion of pharmaceuticals.

**Keywords** Column liquid chromatography · Packing materials · Silsesquioxane · Mercaptopropyl groups · Silanol activity

✉ Qian-Hong Wan  
qhwan@tju.edu.cn

<sup>1</sup> School of Pharmaceutical Science and Technology, Tianjin University, 92 Weijin Road, Tianjin 300072, China

## Introduction

Polysilsesquioxanes, also referred to as organosilicas, are an interesting class of materials with structure characterized by random networks of crosslinked silsesquioxane units with formula  $(RSiO_{1.5})_n$ , where  $R$  is the organic substituent. Compared with inorganic silica ( $SiO_2$ ), these hybrid materials produced by hydrolysis and condensation of organic functional trialkoxysilane monomers exhibit remarkably enhanced chemical, electrical, and mechanical properties, and, therefore, have found widespread applications in functional coatings, microelectronics, and separation membranes [1, 2].

Recently, organosilica-based materials have drawn considerable interest from chromatographers owing to the unique opportunities to tackle the problems inherent in currently predominant silica-based packing materials, such as poor chemical stability and high silanophilic activity [3]. For the past decade, two types of organosilica-based stationary phases have been intensively studied: (a) polymethylsilsesquioxanes (PMSQ)-based monolithic column packings synthesized from methyl silanes by a sol-gel process [4–8] and (b) highly ordered porous materials designated as periodic mesoporous organosilicas (PMOs) prepared from bridged silanes utilizing the same sol-gel approach but in the presence of a surfactant as a structure-directing agent [9–12].

Despite tremendous efforts made to develop organosilica-based chromatographic phases, the number of reports on the synthesis of monodisperse organosilica spherical particles with respective diameters and pore sizes not smaller than 2  $\mu\text{m}$  and 2 nm, intended for use in HPLC, is limited until quite recently. Wan and co-workers adapted the well-known two-step synthetic process combined with a post-synthetic hydrothermal treatment to produce porous

PMSQ particles from methyltrimethoxysilane (MTMS) precursor [13]. Because of their high carbon loading, these highly monodisperse organosilica microspheres obtained show typical reversed-phase chromatographic properties. In contrast to the conventional silica-based reversed-phase packings, the new packing materials display higher hydrothermal stability and lower silanol activity, and thus are potentially useful in the separation of the basic compounds.

To tailor the selectivity of the organosilica packings for specific applications, surface modification on these materials is necessary to provide them with various functionalities for use in different modes of chromatography. Two types of methods are available for this purpose: (a) post-synthetic grafting and (b) co-condensation [2]. The grafting method relies on the condensation reaction of a coupling silane reagent with the surface silanol groups of the substrate, and thus will be effective only when a large number of free silanols are available. This is obviously not the case with the PMSQ material, because the surface silanol groups are mostly replaced by the methyl groups. The co-condensation method involves the hydrolysis and co-condensation of methylalkoxysilanes with one or more organoalkoxysilane(s) in a reaction mixture. As a one-pot synthesis method, co-condensation is considered a viable approach to the surface modification of PMSQ materials, with the density of the functional groups adjusted by varying the ratio of the organosilane precursors in the reaction mixture.

Thiol functionalized packing materials have been the subject of intensive studies over the last three decades mainly because the chemically reactive thiol groups can serve as anchors for attachment of a variety of functional groups [14, 15]. The last decade has witnessed the growing popularity of thiol-ene chemistry in preparation of silica-based chromatographic packings. The radical-mediated thiol-ene reaction has all the desirable features of a click reaction, being highly efficient, simple to execute with no side products, and proceeding rapidly to high yield [16]. Through the thiol-ene click reaction, various silica-based packings have been prepared for reversed-phase chromatography [17], hydrophilic interaction chromatography [18], and mixed mode chromatography [19]. In addition, thiol groups can also be oxidized to sulfonic acid groups for use in ion-exchange chromatography [20].

Here, we report a simple co-condensation method for incorporating thiol groups into the framework of PMSQ microspheres with varying thiol group loadings and a preliminary study on the effects of the thiol loading on the morphology, pore structure, and chromatographic properties of the resulting composite materials. As with PMSQ particles, thiol functionalized PMSQ microspheres were prepared from MTMS and mercaptotrimethoxysilane (MpTMS) precursors by a two-step acid/base process

followed by post-treatment, and characterized using a variety of analytical techniques including SEM, Coulter counter, nitrogen sorption, elemental analysis, spectroscopy, and chromatographic evaluation. The results show that mercaptopropyl contents in the PMSQ can be varied, giving rise to modified materials with enhanced reversed-phase chromatographic properties.

## Experimental

### Chemicals

MTMS, MpTMS were purchased from Wuda Silicone Materials (Wuhan, China). Hydrochloric acid, ethanol, methanol, ammonia (25 wt%), and toluene were purchased from Concord Chemical Reagents (Tianjin, China). Uracil, toluene, ethylbenzene, quinizarin, and amitriptyline were obtained from various sources and used without further purification. Deionized water was obtained from a Milli-Q Synthesis A10 water purification system.

### Synthesis

Mercaptopropyl functionalized PMSQ particles were prepared by following a method previously reported [13]. In a typical experiment for preparation of particles from a reaction mixture containing 20% (w/w) MpTMS, 8 g of MpTMS and 32 g of MTMS were added to 200 mL of deionized water containing 0.4 mL of hydrochloric acid solution, which was placed in a 250-mL reaction flask equipped with a Teflon-coated stirrer. The reaction mixture was agitated at room temperature for 6 h to produce a clear solution. The solution was then basified with 15  $\mu$ L of ammonia. The initially translucent solution turned cloudy within 3 min, and quickly became fully opalescent due to the formation of particles. Agitation was stopped to allow the reaction to continue at a standstill for 5 h at 30 °C. The resulting particles were isolated by centrifugation and washed thoroughly using ethanol and water. The particles were then suspended in 200 mL of 80% ethanol containing 10% (v/v) of ammonia and heated at reflux for 12 h. At the end of alkaline-heat treatment, the particles were isolated, washed, and dried 50 °C overnight. Pure PMSQ and a series of Mp(X)-PMSQ (*X* is referred to the weight percentage of the MpTMS in the reaction mixture) were synthesized essentially in the same way as for Mp(20)-PMSQ except that the *X* value was varied.

### Characterization

SEM images of the particle samples were taken using a Nova NanoSEM 430 scanning electron microscope from

FEI (Hillsboro, Oregon, USA). The mean particle sizes ( $D_{50}$ ) and size distribution ( $D_{90}/D_{10}$ ) were determined using a Beckman Coulter Multisizer 3 (Brea, CA, USA) equipped with a 100  $\mu\text{m}$  orifice glass tube. Porosity measurements were performed by nitrogen adsorption–desorption at 77 K using a Quantachrome Nova 3000 surface area analyzer (Boynton Beach, FL, USA). The specific surface area ( $S_{\text{BET}}$ ), the total pore volume ( $V_p$ ), and pore diameter ( $D_p$ ) were calculated using the multi-point BET equation, a single condensation point at  $P/P_0 = 0.995$ , and BJH (Barrett, Joyner, and Halenda) model, respectively [18]. The carbon contents (% C) and sulfur contents (% S) of the particles were measured using a Vario Micro Cube from Elementar Analysen systemene (Hanau, Germany). Solid-state  $^{29}\text{Si}$  and  $^{13}\text{C}$  CP/MAS NMR spectra were measured on a Varian InfinityPlus-300 MHz spectrometer (Palo Alto, CA, USA) equipped with a 7.5 mm double-resonance MAS probe at a spinning rate of 5 kHz. The  $^{29}\text{Si}$  spectra were recorded at a pulse repetition time of 5 s, a contact time of 10 ms, and a frequency of 59.6 MHz. For  $^{13}\text{C}$  spectra, a pulse repetition time of 5 s, a contact time of 5 ms, and a frequency of 75.4 MHz were used. Characteristic frequencies of the functional groups on the particles were measured in KBr disks using a TENSOR Fourier transform infrared spectroscope (Bruker, Germany). The residual silanol content of the organosilica particles was measured by conductometric titration. The particle sample (approximately 0.1 g) was suspended in a 10 mL of 0.1 M NaOH in which 3 mL of EtOH was added. The mixture was stirred for 30 min and titrated with 0.1 M HCl. The change in electric conductivity was followed using an Accumet Basic AB30 conductometer from Fisher Scientific (Bridgewater, NJ, USA). The volumes consumed to reach the minimum in conductivity were used to calculate the concentration of acidic groups in the sample.

### Chromatographic Evaluation

Organosilica particles were slurry packed into an HPLC column (150  $\times$  4.6 mm I.D.) under constant pressure of 400 bar using isopropanol and methanol as slurry and displacement solvents, respectively. Testing of the packed columns was conducted on an Agilent 1200 series HPLC system equipped with a vacuum degasser, a quaternary pump, an autosampler, a column oven, and a variable wavelength UV detector from Agilent Technologies (Palo Alto, CA, USA). A chromatographic data system from the manufacturer, ChemStation version B 03.01, was used for data acquisition and instrument control. Except where specified, chromatographic analyses were carried out under the following standard conditions: column temperature 25  $^{\circ}\text{C}$ , flow rate 1.0 mL  $\text{min}^{-1}$ , and detection wavelength 254 nm.

The mobile phases composed of methanol/30 mM sodium phosphate buffer with pH adjusted from 2 to 13 (80:20 v/v) were used to determine the retention factors ( $k$ ) of a basic probe benzyltriethylammonium chloride at various pH values. The dissociation constant,  $pK_a$ , of the silanol/thiol groups was calculated by the following formula [21]:

$$k = A + \{B/[1 + 10^{(pK_a - \text{pH})}]\} \quad (1)$$

where  $A$  and  $B$  correspond to the retention factors of the probe molecule on the packing with undissociated and fully dissociated silanol/thiol groups.

The mobile phases composed of methanol/30 mM phosphate buffer (pH 7.0) (80:20 v/v) were used for chromatographic evaluation of the packed columns using a testing procedure developed by Sander and Wise [22]. A standard mixture containing uracil, toluene, ethylbenzene, quinizarin, and amitriptyline was used to determine the hydrophobicity, methylene selectivity, metal, and silanol activities of the packing materials.

## Results and Discussion

### Morphology and Sizes of Particles

Spherical shape and uniform size are desirable traits of an ideal packing material as they lead to a more uniform packing bed and thus a highly efficient column. SEM micrographs of synthesized PMSQ and Mp(X)-PMSQ microspheres (Fig. 1) clearly show that they are spherical in morphology and relatively uniform in size. However, the particle size distributions determined by Coulter counter appear multimodal (Fig. 2) with a small fraction of particles about 1–2  $\mu\text{m}$  larger. This type of size distribution has been observed previously by Miller et al. [23] and the formation of larger particles was attributed to two or more smaller droplets coalescing together at an earlier stage of particle formation. The mean particle sizes ( $D_{50}$ ) and spans of the size distribution ( $D_{90}/D_{10}$ ) of the microspheres are shown in Table 1. The  $D_{50}$  and  $D_{90}/D_{10}$  values were in the range of 5.21–8.11 and 1.22–1.47  $\mu\text{m}$ , respectively. Due to the fact that particle size is sensitive to the synthetic conditions used, no conclusion could be drawn about the role of mercaptopropyl loading in controlling particle size and size distribution.

Particle size distribution has profound effects on the permeability and uniformity of a particle-packed column [24]. As a rule of thumb, the packing materials with  $D_{90}/D_{10}$  less than 1.6 are generally preferred to produce a homogenous packing bed with low mass transfer resistance [25]. Conventional methods for the preparation of porous silica or organic–inorganic silica spheres are based on

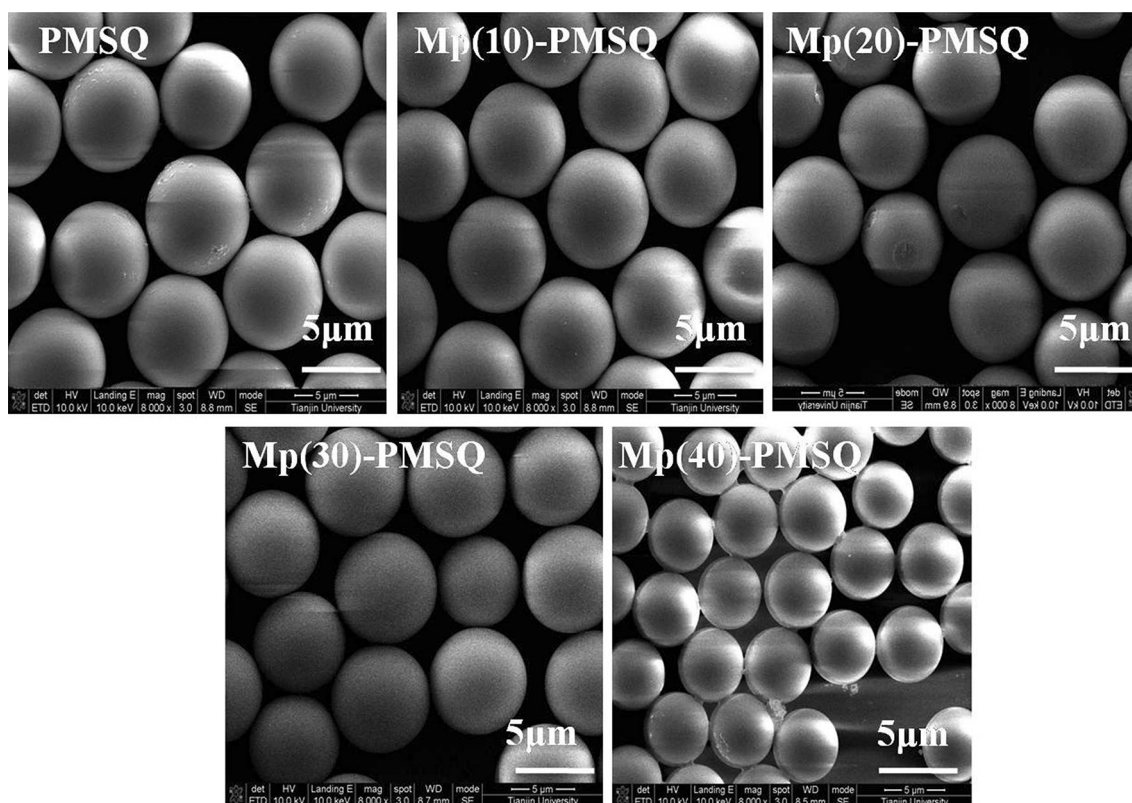


**Fig. 1** SEM images of pure and mercaptopropyl functionalized PMSQ particles

emulsification of siloxane oligomers in an ethanol–water mixture by vigorous stirring followed by alkaline catalyzed polycondensation reaction [26, 27]. Due to the beading process by stirring, the particle size distribution is relatively broad with typical  $D_{90}/D_{10}$  values in the range of 2.5–4.0 and, therefore, has to be subjected to sizing. The as-synthesized mercaptopropyl functionalized PMSQ particles have  $D_{90}/D_{10}$  values well below 1.6, making the tedious post-synthetic size classification procedure obsolete.

### Surface Area and Pore Structure

The rate of mass transfer of solute molecules into and out of the stationary phase is controlled mainly by their diffusion within the porous particles that constitute the column bed [24]. As such, the pore structure of the packing is important with respect to the column efficiency. A nitrogen sorption technique was employed to evaluate the pore structure parameters of pure and functionalized PMSQ microspheres. The adsorption and desorption isotherms exhibited by PMSQ and functionalized materials with  $X$  up to 20 (Fig. 3a) are fairly typical of mesoporous solids (type IV isotherm [28]). However, type I isotherm of microporous material and type II isotherm of nonporous solid were observed for Mp(30)- and Mp(40)-PMSQ

particles, respectively, indicating a transition in pore structure with increasing mercaptopropyl loading. The pronounced change is observed again in pore size distribution (Fig. 3b), where the mean pore size drops off drastically for the Mp(30)- and Mp(40)-PMSQ particles. The specific surface area ( $S_{\text{BET}}$ ), pore volume ( $V_p$ ), and the average pore sizes ( $D_p$ ) determined by the BJH method for mesoporous materials and the NLDFT method [29] for Mp(30)- and Mp(40)-PMSQ particles, respectively, are presented in Table 1. Evidently, the mercaptopropyl loading has profound influence on the pore structure parameters, with BET surface area, pore volume, and pore size decreasing from  $754 \text{ m}^2 \text{ g}^{-1}$ ,  $0.72 \text{ mL g}^{-1}$ , and  $3.83 \text{ nm}$  for PMSQ to  $48 \text{ m}^2 \text{ g}^{-1}$ ,  $0.042 \text{ mL g}^{-1}$ , and  $2.58 \text{ nm}$  for Mp(40)-PMSQ particles. It is worth mentioning that the calculated pore structure parameters especially the pore size are not absolute, owing to assumptions inherent in the method and sensitivity to the synthesis conditions, but enable comparison of the data obtained for functionalized particles to be made. Experimental studies are currently underway to gauge the inter- and intra-batch reproducibility.

A knowledge of the mechanism behind the formation and growth of the particles is necessary to understand the observed effects of the mercaptopropyl loading on pore structure. Many studies have been carried out to elucidate

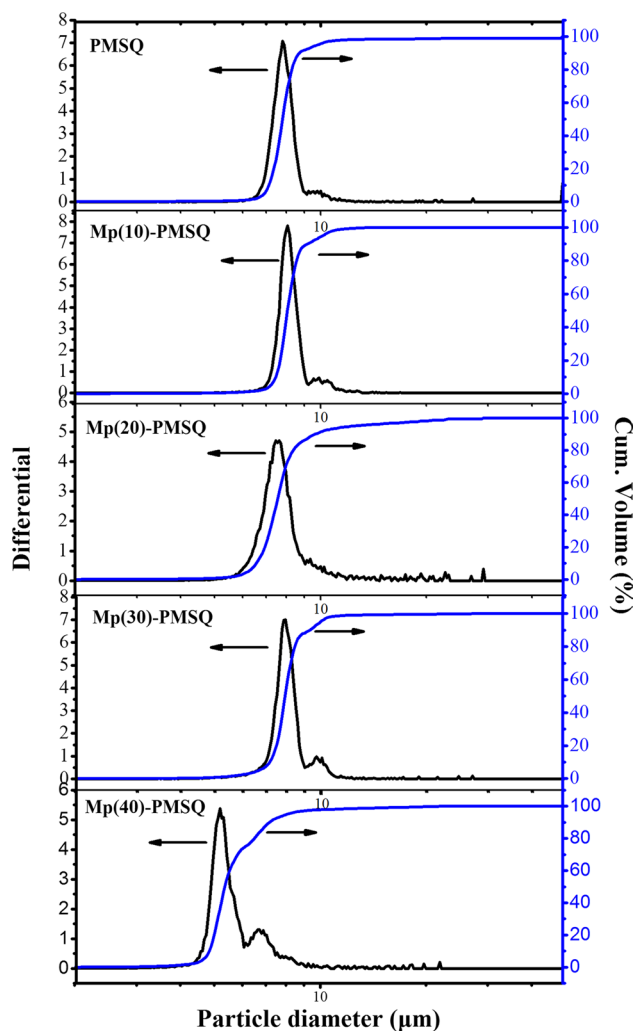


**Fig. 2** Particle size distribution of pure and mercaptopropyl functionalized PMSQ particles

the origin of porosity in particles derived from organosilanes. Most of the experimental observations can be accounted for by the aggregation/monomer or oligomer addition model proposed by Matsoukas and Guilari [30] and modified by others [31, 32]. According to this concept, monomers are hydrolyzed and condensed, resulting in oligomers of varying lengths and structures [33–35]. These oligomers are then condensed under alkaline conditions to produce primary nuclei. These small nuclei further aggregate to form larger particles with porous structures. At the same time, oligomers may be adsorbed or trapped onto the particle surface and block the entrance or possibly inner part of the interparticle pores. This is particularly the case for monomers with slow hydrolysis and condensation rates, giving rise to the oligomers at concentrations below the threshold for the colloid formation. The decrease in the porosity observed with increasing mercaptopropyl loading is thus attributed to the pore

**Table 1** Physicochemical characterization of pure and mercaptopropyl functionalized PMSQ microspheres

Material (mole fraction of MpTMS) <sup>c</sup>	Particle size distribution		Pore structure		Chemical composition		Functional groups			
	$D_{50}$ ( $\mu\text{m}$ )	$D_{90}/D_{10}$	$S_{\text{BET}}$ ( $\text{m}^2 \text{g}^{-1}$ )	$V_p$ ( $\text{mL g}^{-1}$ )	$D_p$ (nm)	% C measured (theoretical) <sup>d</sup>	% S measured (theoretical) <sup>d</sup>	$-\text{CH}_3$ ( $\text{mmol g}^{-1}$ )	$-\text{CH}_2\text{SH}$ ( $\text{mmol g}^{-1}$ )	Mole fraction of thiol group, $Y$
PMSQ (0)	7.84	1.22	754	0.72	3.83 <sup>a</sup>	16.53 (17.9)	0.01 (0)	11.81	0	0
Mp(10)-PMSQ (0.07)	8.11	1.23	702	0.60	3.85 <sup>a</sup>	16.83 (18.65)	3.01 (3.15)	9.20	0.94	0.093
Mp(20)-PMSQ (0.15)	7.49	1.47	641	0.52	3.83 <sup>a</sup>	17.16 (19.4)	6.00 (6.32)	8.69	1.87	0.177
Mp(30)-PMSQ (0.23)	7.93	1.30	359	0.17	2.34 <sup>b</sup>	19.21 (20.3)	9.01 (9.10)	7.52	2.83	0.273
Mp(40)-PMSQ (0.32)	5.21	1.38	48	0.042	2.58 <sup>b</sup>	19.25 (21.2)	10.23 (11.88)	6.44	3.20	0.330

<sup>a</sup>The mesopore size is calculated by the BJH method

<sup>b</sup>The micropore size is calculated by the DFT method

<sup>c</sup>The mole fraction of MpTMS in the reaction mixture

<sup>d</sup>The theoretical carbon and sulfur contents calculated according to the formula  $(\text{MpsSiO}_{1.5})_x(\text{MeSiO}_{1.5})_y(\text{MeSiO}_{1.5})_{(1-y)}$ , where  $Y$  is the molar fraction of MpTMS in the reaction mixture

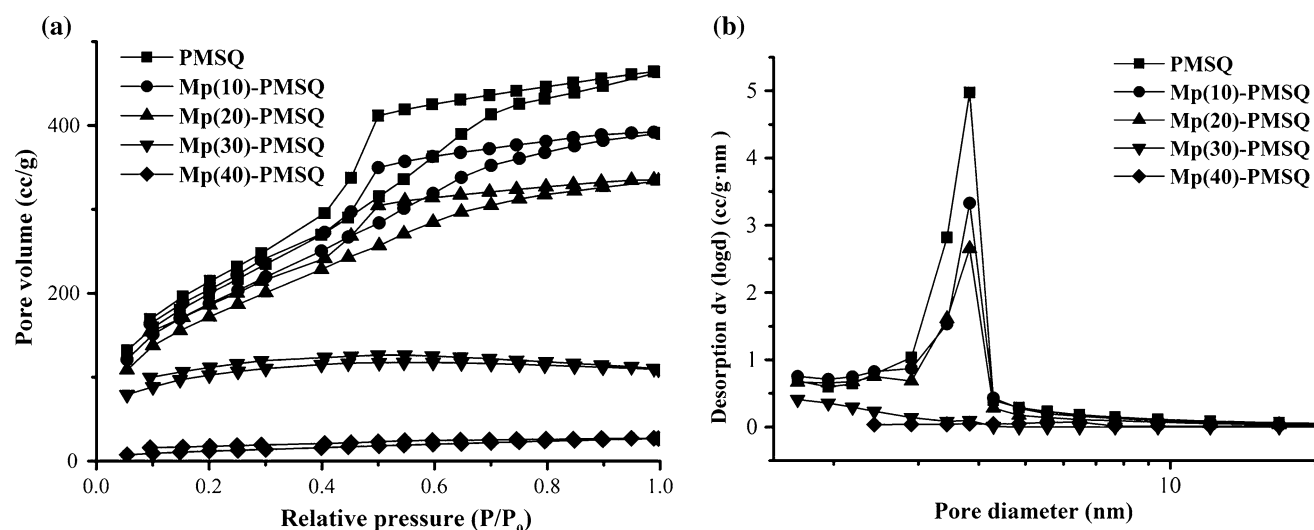


**Fig. 3** **a** Nitrogen sorption isotherms and **b** pore size distributions of pure and mercaptopropyl functionalized PMSQ particles

clogging effect arising from the entrapment of organofunctionalized oligomers.

### Spectroscopic Characterization

The carbon and sulfur percentages of organosilica microspheres determined by the elemental analysis are presented in Table 1 and compared with those calculated based on assumption that a complete condensation occurs with the precursors. Both carbon and sulfur contents increase with the mercaptopropyl loading. However, the measured values do not always agree with the theoretical ones, and some of the differences appear to be quite large. One plausible explanation is associated with the presence of surface silanol groups, which were not taken into account in the assumption. The measured mole fractions of mercaptopropyl to methyl groups in the products were slightly higher than those calculated based on the ratios of precursors in the reaction mixture, suggesting that both precursors were converted without any pronounced discrimination.

Solid-state NMR spectra (Fig. 4) show the presence of both Si–O–Si and Si–C linkages. Although the resonances from the methyl silica are overlapped with those from mercaptopropyl silica, peaks characteristic of organosilica species is clearly visible in the  $^{29}\text{Si}$  spectrum (Fig. 4a) for Mp(20)-PMSQ particles. Peaks at  $-57.6$  and  $-66.5$  ppm were assigned, respectively, to hydroxylated  $\text{T}^2$  and fully condensed  $\text{T}^3$  species [36]. The formation of  $\text{T}^1$  and  $\text{T}^0$  species is insignificant, suggesting that although the condensation is not fully completed, no unreacted precursor monomer is present.  $^{13}\text{C}$  spectrum (Fig. 4b) exhibits carbon resonance characteristic of the corresponding organic groups. No intense peak characteristic of residual methoxy

groups is seen in the spectrum, confirming that these groups are almost completely hydrolyzed during the reaction, and OH groups are the only functional groups retained without condensation in the  $\text{T}^2$  species.

The particle samples were further characterized by infrared spectroscopy [14, 36]. As shown in Fig. 5a, the broad peak near  $3500\text{ cm}^{-1}$  is caused by the hydroxyl O–H stretching vibration, confirming the presence of the silicon species with hydroxyl groups. The absorption bands at around  $2950\text{ cm}^{-1}$  are assigned to the asymmetric and symmetric methyl and methylene group vibrations. The absorption peak in the range  $2300\text{--}2500\text{ cm}^{-1}$  is characteristic of thiol groups. Figure 5b provides magnified views of the spectra in the range  $2200\text{--}3200\text{ cm}^{-1}$ . Absorption intensities of both the thiol at  $2300\text{ cm}^{-1}$  and methylene groups at  $2925\text{ cm}^{-1}$  increase with the mercaptopropyl loading in the particles.

### Concentration and Acidity of Surface Silanol and Thiol Groups

Spectroscopic studies have demonstrated the existence of isolated silanols in pure and functionalized PMSQ particles. The next problem that arises is to determine the surface hydroxyl and/or thiol group concentration,  $\alpha_{\text{OH}/\text{SH}}$ . Various experimental techniques can be used for this purpose, in which chemical methods permit the most precise measurement of  $\alpha_{\text{OH}/\text{SH}}$  because of its well-known stoichiometry and easy detection [37]. In this work, conductometric titration was employed to measure the acidic surface groups for its simplicity and convenience. As shown in Table 2, the silanol concentration of about  $0.13\text{ }\mu\text{mol m}^{-2}$  was found for PMSQ and the surface group (silanol + thiol)

**Fig. 4** Solid-state  $^{29}\text{Si}$  NMR (a) and  $^{13}\text{C}$  NMR spectrum (b) of Mp(20)-PMSQ particles

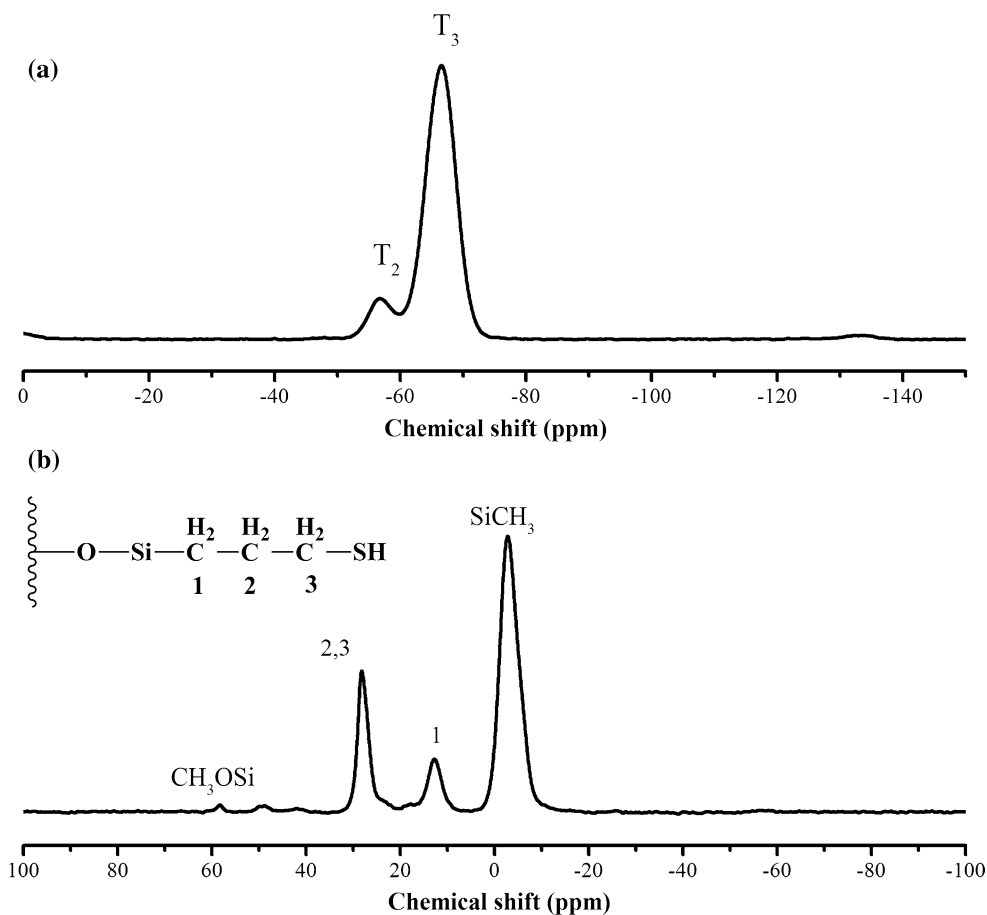
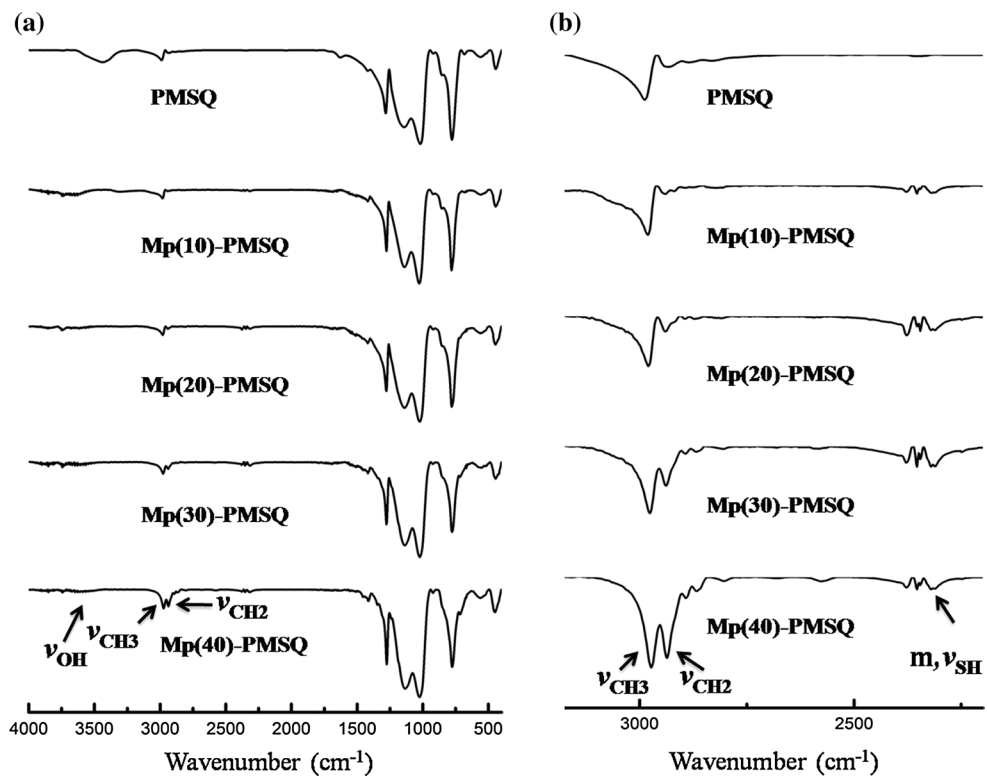


**Fig. 5** Infrared spectra of pure and mercaptopropyl functionalized PMSQ particles



concentrations of 0.15–2.48  $\mu\text{mol m}^{-2}$  were obtained for Mp(X)-PMSQ microspheres. During the titration experiments, the use of the alkaline titrate concentrations was carefully chosen to avoid erosive damages to the particles. Under these conditions, some very weak acidic groups may not be dissociated. As a result, the number of surface acidic groups may be underestimated and the data presented here represent the lower limits only.

The dissociation constants ( $\text{p}K_{\text{a}}$ ) of the acidic silanols or thiols for organosilica microspheres were determined by chromatography using benzyltriethylammonium chloride as a probe. The benzyltriethylammonium cations interact electrostatically with dissociated silanol/thiol groups, giving rise to a pronounced increase in retention. By examining the retention factor of the benzyltriethylammonium chloride as a function of the mobile phase pH, the  $\text{p}K_{\text{a}}$  values of acidic groups can be calculated for the organosilica particles. As shown in Table 2, the  $\text{p}K_{\text{a}}$  value of about 14 was found for PMSQ, whereas slightly lower values (about 12) were obtained for the functionalized particles.

Vast majority of  $\text{p}K_{\text{a}}$  values for silanol or thiol groups in the literature are in the range of 2–7 or 8–10, well below the data we obtained for organosilica particles. However, exceptionally, high  $\text{p}K_{\text{a}}$  values for both silanol and thiol groups have been reported as well. With incompletely condensed silsesquioxanes as models for silica surface silanols, Duchateau et al. [38] reported the  $\text{p}K_{\text{a}}$  values of 9.6–11.1 for silsesquioxane silanols. It has been shown that alkyl substitution, intramolecular hydrogen bonding, and hydrophobic environment all lead to a pronounced decrease in acidity. Mercaptopropyl and methyl substituents are electron donating groups, making the oxygen atom in the hydroxyl group more negative. The random network structure of the polysilsesquioxanes provides ample intramolecular hydrogen bonding opportunities, leading to acidities even lower than in silsesquioxanes. A further reduction in acidity is expected for silanols that are buried in the surrounding hydrophobic methyl and mercaptopropyl groups.

The interpretation of the  $\text{p}K_{\text{a}}$  values is complicated by the presence of thiol groups which may have  $\text{p}K_{\text{a}}$  values close to those of silanols. Experimental measurements of

thiol  $\text{p}K_{\text{a}}$  values have been actively pursued for enzymes in which the acidity of thiols has a strong influence on catalysis. According to Chivers et al. [39], cysteine residues in thioredoxin have  $\text{p}K_{\text{a}}$  values varying from 6.16 to greater than 11, depending on their microenvironments. Since we were unable to determine the acidity of thiols on the highly hydrophobic surface of polysilsesquioxane independently, the question remains open whether the measured  $\text{p}K_{\text{a}}$  values for mercaptopropyl functionalized particles actually correspond to silanols or thiols.

## Retention Characteristics

The incorporation of mercaptopropyl groups raises the carbon loading and thus hydrophobicity of the resulting composite materials. The retention characteristics of the mercaptopropyl functionalized PMSQ particles were evaluated using a testing procedure developed by Sander and Wise [22]. A testing mixture containing uracil, toluene, ethylbenzene, quinizarin, and amitriptyline was used to determine the hydrophobicity, methylene selectivity, metal, and silanol activities of the packing material. Figure 6 shows separations of the test mixture on pure PMSQ and a series of Mp(X)-PMSQ packings. The test compounds were eluted in the order of uracil, toluene/quinizarin, ethylbenzene, and amitriptyline on the PMSQ packing. An increase in retention of the analyte with mercaptopropyl loading was observed for the functionalized particles.

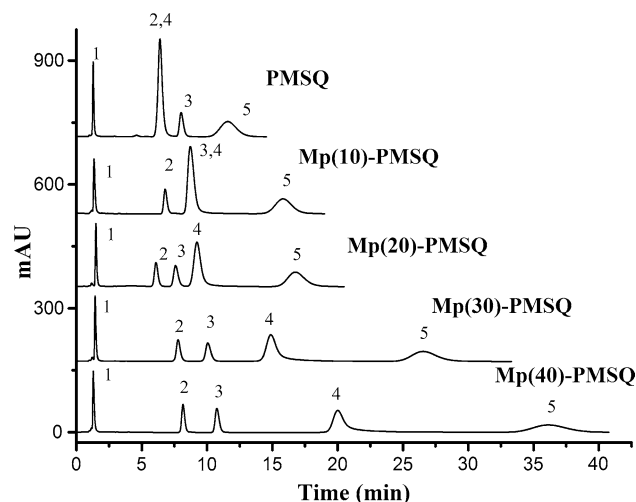


**Fig. 6** Separation of test compounds on column packed with **a** PMSQ, **b** Mp(10)-PMSQ, **c** Mp(20)-PMSQ, **d** Mp(30)-PMSQ, and **e** Mp(40)-PMSQ microspheres. Column 150  $\times$  4.6 mm ID, column temperature 25  $^{\circ}\text{C}$ , mobile phase 80:20 (v/v) methanol/30 mM phosphate buffer (pH 7), flow rate 1  $\text{mL min}^{-1}$ , detection wavelength 254 nm. Solutes: (1) uracil, (2) toluene, (3) ethylbenzene, (4) quinizarin, and (5) amitriptyline

**Table 2** Concentrations ( $\alpha_{\text{OH/SH}}$ ) and dissociation constants ( $\text{p}K_{\text{a}}$ ) of silanol/thiol groups in pure and thiol functionalized PMSQ microspheres

Material	$\alpha_{\text{OH/SH}}$ ( $\mu\text{mol m}^{-2}$ )	$\text{p}K_{\text{a}}$
PMSQ	0.13	14.5
Mp(10)-PMSQ	0.15	11.9
Mp(20)-PMSQ	0.20	11.5
Mp(30)-PMSQ	0.34	11.6
Mp(40)-PMSQ	2.48	11.6



The retention of the solute on mercaptopropyl functionalized packings may be understood in terms of the well-known interphase model [40]. Key to this model is that interfaces are formed between two mutually immiscible phases when brought into intimate contact and can be depicted as a surface formed at the point of contact between the two phases. Interactions with the stationary phase may occur at the surface of the stationary phase (adsorption), or the sample may cross the interface and interact with the bulk stationary phase (partition). It is a favorable change in free energy for adsorption or partition that explains whether retention is the result of interfacial interactions or solvation. According to this model, the reversed-phase system may be considered as partition system, where the effective volume of the stationary phase,  $V_s$ , is expressed as

$$V_s = S_{\text{BET}} \times d_s \quad (2)$$

where  $S_{\text{BET}}$  is the specific surface area of the packings in the column and  $d_s$  is the effective film thickness of the bonded material and any solvent that may be absorbed in the stationary phase.

By definition, the retention factor,  $k$ , of a solute is given by the expression:

$$k = K \frac{V_s}{V_m} \quad \text{or} \quad k = K \frac{S_{\text{BET}} \times d_s}{V_m} \quad (3)$$

where  $K$  is the distribution coefficient of the solute between the two phases and  $V_m$  is the effective volume of the mobile phase.

Based on Gibbs free energy additivity principle,  $K$  can be correlated to the mole fraction of the mercaptopropyl groups in the packing,  $Y$ , by the following equation:

$$\log K = (1 - Y) \log K_{\text{PMSQ}} + Y \log K_{\text{PMpSQ}} \quad (4)$$

where  $K_{\text{PMSQ}}$  and  $K_{\text{PMpSQ}}$  are the distribution coefficients of the solute with pure methyl- and mercaptopropyl-based organosilica packings, respectively.

Accordingly,  $d_s$  is related to  $Y$  by the following expression:

$$d_s = (1 - Y)d_{s,\text{PMSQ}} + Yd_{s,\text{PMpSQ}} \quad (5)$$

where  $d_{s,\text{PMSQ}}$  and  $d_{s,\text{PMpSQ}}$  are the film thickness on the surfaces of the methyl and mercaptopropyl phases, respectively.

By substituting Eqs. (4) and (5) into Eq. (3) and rearranging, we arrive at

$$\log k \frac{V_m}{S_{\text{BET}}} = \log K_{\text{PMSQ}} + Y \log \frac{K_{\text{PMpSQ}}}{K_{\text{PMSQ}}} + \log [d_{s,\text{PMSQ}} + Y(d_{s,\text{PMpSQ}} - d_{s,\text{PMSQ}})] \quad (6)$$

Since the dependence of  $K$  on  $Y$  is exponential, whereas the dependence of  $V_s$  on  $Y$  is linear, it seems reasonable to omit the contribution of the increasing  $V_s$  due to the

incorporated mercaptopropyl groups. Equation (6) can be simplified to

$$\log k \frac{V_m}{S_{\text{BET}}} = \log K_{\text{PMSQ}} d_{s,\text{PMSQ}} + Y \left( \log \frac{K_{\text{PMpSQ}}}{K_{\text{PMSQ}}} \right) \quad (7)$$

Thus, a linear relationship between  $\log(kV_m/S_{\text{BET}})$  and  $Y$  is expected for a given system at constant eluent composition and temperature, with an intercept of  $\log(K_{\text{PMSQ}}d_{s,\text{PMSQ}})$  and a slope of  $\log(K_{\text{PMpSQ}}/K_{\text{PMSQ}})$ .

As shown in Fig. 7, the effect of mole fraction of mercaptopropyl groups on the normalized retention factor appears to be much more complicated than that based on energy consideration as the  $\log(kV_m/S_{\text{BET}})$  values do not fit the straight line over the  $Y$  range investigated. The unexpected abrupt rise in the curve at about  $Y = 0.2$  may be caused by the changing surface structure, in which more mercaptopropyl groups are exposed to the surface, leading to greater increase in retention. The mercaptopropyl groups exist as internal and external fractions and only external fractions contribute to the solute retention. The total and surface thiol contents can be measured by elemental analysis and oxidative titration, respectively. Thus, further experimentation regarding accessible mercaptopropyl fractions is necessary to rationalize the exceptional retention behavior observed.

The mercaptopropyl functionalized organosilica packings show moderate column efficiency, with typical numbers of theoretical plates ( $N \text{ m}^{-1}$ ) of about 16,000 for ethylbenzene. The methylene selectivity ( $k_{\text{ethylbenzene}}/k_{\text{toluene}}$ ) increases slightly from 1.34 for PMSQ particles to 1.38 for Mp(40)-PMSQ packing. Relatively symmetric peaks observed for quinizarin and amitriptyline indicate low

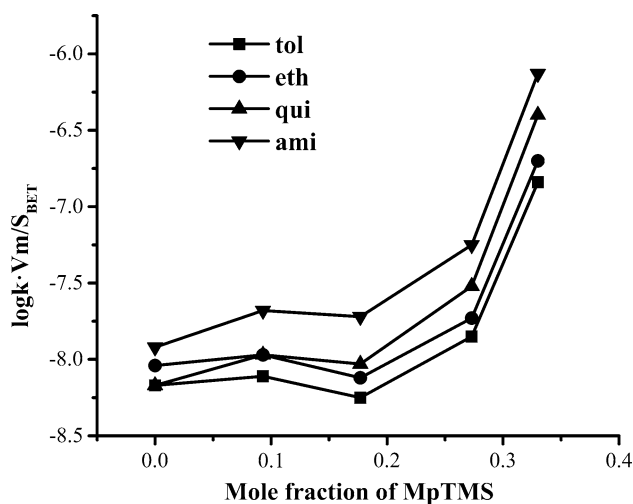


**Fig. 7** Normalized retention factor [ $\log(kV_m/S_{\text{BET}})$ ] of the testing compounds as a function of mole fraction ( $Y$ ) of functional groups in pure and mercaptopropyl functionalized PMSQ packings

metal and alkaline activities as one would expect for low acidity packing materials. At its current state, the new packing material cannot compete with silica-based packings in terms of column efficiency. Among many factors that influence the column efficiency, micropores present in these particles and incompact packed beds are believed mainly responsible for broad peaks observed. Future development should focus more on pore enlargement and optimization of packing conditions.

## Conclusions

Co-condensation has been used to synthesize a series of mercaptopropyl functionalized polymethylsilsesquioxane microspheres for use as novel chromatographic packing materials. The results obtained over a range of mercaptopropyl to methyl ratios show that incorporation of mercaptopropyl functional groups has profound effects on the particle formation and pore structure. A transition from mesoporous to microporous and nonporous structures occurs when mercaptopropyl silane in the reaction mixture exceeds about 30 wt%. The observed decrease in surface area, pore volume, and pore size is primarily attributed to the pore clogging effect arising from the entrapment of organofunctionalized oligomers. The thiol functionalized particles display low acidity, presumably due to a concerted action of electron donating ability of the substituents, intramolecular hydrogen bonding and low dielectric microenvironment. Furthermore, they exhibit enhanced reversed-phase retention properties, corresponding to an increase in carbon loading. A retention model is proposed to account for the dependence of the retention factor of the solute on mole fraction of mercaptopropyl group in the composite particles. As an intermediate phase, the thiol functionalized PMSQ can be further modified by thiol-ene click reaction to provide versatile and multifunctional packing materials for challenging problems in pharmaceutical analysis.

## Compliance with Ethical Standards

**Conflict of interest** Authors declare no conflict of interest.

**Ethical approval** This article does not contain any studies with human participants or animals performed by any of the authors.

## References

- Sanchez C, Belleville P, Popall M, Nicole L (1995) Applications of advanced hybrid organic–inorganic nanomaterials: from laboratory to market. *Chem Soc Rev* 40:696–753
- Hoffmann F, Froba M (2011) Vitalising porous inorganic silica networks with organic functions—PMOs and related hybrid materials. *Chem Soc Rev* 40:608–620
- Kanamori K, Nakanishi K (2011) Controlled pore formation in organotrialkoxysilane-derived hybrids: from aerogels to hierarchically porous monoliths. *Chem Soc Rev* 40:754–770
- Kanamori K, Yonezawa H, Nakanishi K, Hirao K, Jinnai H (2004) Structural formation of hybrid siloxane-based polymer monolith in confined spaces. *J Sep Sci* 27:874–886
- Dong HJ, Brook MA, Brennan JD (2005) A new route to monolithic methylsilsesquioxanes: gelation behavior of methyltrimethoxysilane and morphology of resulting methylsilsesquioxanes under one-step and two-step processing. *Chem Mater* 17:2807–2816
- Dong H, Brennan JD (2006) Controlling the morphology of methylsilsesquioxane monoliths using a two-step processing method. *Chem Mater* 18:541–546
- Popp M, Sulyok M, Rosenberg E (2007) Chromatographic characterisation of a novel type of monolithic methylsilsesquioxane-based HPLC column. *J Sep Sci* 30:2888–2899
- Laschober S, Rosenberg E (2008) Chromatographic characterisation of monolithic capillary columns for liquid chromatography based on methyltrimethoxysilane as sole precursor. *J Chromatogr A* 1191:282–291
- Kim DJ, Chung JS, Ahn WS, Kang GW, Cheong WJ (2004) Morphology control of organic–inorganic hybrid mesoporous silica by microwave heating. *Chem Lett* 33:422–423
- Rebbin V, Schmidt R, Froba M (2006) Spherical particles of phenylene-bridged periodic mesoporous organosilica for high-performance liquid chromatography. *Angew Chem Int Ed* 45:5210–5214
- Zhu G, Yang Q, Jiang D, Yang J, Zhang L, Li Y, Li C (2006) Synthesis of bifunctionalized mesoporous organosilica spheres for high-performance liquid chromatography. *J Chromatogr A* 1103:257–264
- Zhang Y, Jin Y, Dai P, Hu H, Yu D, Ke Y, Liang X (2009) Phenylene-bridged hybrid silica spheres for high performance liquid chromatography. *Anal Methods* 1:123–127
- Wan QH, Huo ZX, Chen L (2016) Monodispersed porous polysilsesquioxane microspheres and their preparation. In: Chinese patent CN106084228A. <http://www.google.com/patents/CN106084228A>. Published date 09 Nov 2016
- Norma M, Scully NM, O’Sullivan GP, Healy LO, Glennon JD, Dietrich B, Albert K (2007) Preparation of a mercaptopropyl bonded silica intermediate in supercritical carbon dioxide: synthesis, characterisation and chromatography of a quinine based chiral stationary phase. *J Chromatogr A* 1156:68–74
- Dabre R, Schwämmle A, Lämmerhofer M, Lindner W (2009) Statistical optimization of the silylation reaction of a mercaptosilane with silanol groups on the surface of silica gel. *J Chromatogr A* 1216:3473–3479
- Hoyle CE, Bowman CN (2010) Thiol-ene click chemistry. *Angew Chem Int Ed* 49:1540–1573
- Ruderisch A, Iwanek W, Pfeiffer J, Fischer G, Albert K, Schurig V (2005) Synthesis and characterization of a novel resorcinarene-based stationary phase bearing polar headgroups for use in reversed-phase high-performance liquid chromatography. *J Chromatogr A* 1095:40–49
- Shen A, Guo Z, Cai X, Xue X, Liang X (2012) Preparation and chromatographic evaluation of a cysteine-bonded zwitterionic hydrophilic interaction liquid chromatography stationary phase. *J Chromatogr A* 1228:175–182
- Lämmerhofer M, Nogueira R, Lindner W (2011) Multi-modal applicability of a reversed-phase/weak-anion exchange material in reversed-phase, anion-exchange, ion-exclusion, hydrophilic interaction and hydrophobic interaction chromatography modes. *Anal Bioanal Chem* 400:2517–2530

20. Horak J, Lindner W (2008) Contribution of sulfonyl–aromatic and sulfonic acid–aromatic interactions in novel sulfonyl/sulfonic acid-embedded reversed phase materials. *J Chromatogr A* 1191:141–156
21. Mendez A, Bosch E, Roses M, Neue UD (2003) Comparison of acidity of residual silanol groups in several liquid chromatography columns. *J Chromatogr A* 986:33–44
22. Sander LC, Wise SA (2003) A new standard reference material for column evaluation in reversed-phase liquid chromatography. *J Sep Sci* 26:283–294
23. Miller CR, Vogel R, Surawski PPT, Jack KS, Corrie SR, Trau M (2005) Functionalized organosilica microspheres via a novel emulsion-based route. *Langmuir* 21:9733–9749
24. Knox JH (2002) Band dispersion in chromatography—a universal expression for the contribution from the mobile zone. *J Chromatogr A* 960:7–18
25. Hohenesche CF, Ehwald V, Unger KK (2004) Development of standard operation procedures for the manufacture of *n*-octadecyl bonded silicas as packing material in certified reference columns for reversed-phase liquid chromatography. *J Chromatogr A* 1025:177–187
26. Unger K, Scharf B (1976) Controlled porosity silica supports from hydrolytic polycondensation reaction of poly(ethoxysiloxane). *J Colloid Interface Sci* 55:377–380
27. Wyndham KD, O’Gara JE, Walter TH, Glose KH, Lawrence NL, Alden BA, Izzo GS, Hudalla CJ, Iraneta PC (2003) Characterization and evaluation of C<sub>18</sub> HPLC stationary phases based on ethyl-bridged hybrid organic/inorganic particles. *Anal Chem* 75:6781–6788
28. Gregg SJ, Sing KSW (1982) Adsorption, surface area and porosity. Academic Press, New York
29. Thommes M (2007) Textural characterization of zeolites and ordered mesoporous materials by physical adsorption. *Stud Surf Sci Catal* 168:495–523
30. Matsoukas T, Guilari E (1988) Dynamics of growth of silica particles from ammonia-catalyzed hydrolysis of tetra-ethyl-orthosilicate. *J Colloid Interface Sci* 124:252–261
31. Carcouet CCMC, van de Put MWP, Mezari B, Magusin PCMM, Laven J, Bomans PHH, Fridrich H, Esteves ACC, Sommerdijk NAJM, van Benthem RATM, de With AC (2014) Nucleation and growth of monodisperse silica nanoparticles. *Nano Lett* 14:1433–1438
32. Li S, Wan Q, Qin Z, Fu Y, Gu Y (2014) Understanding Stober silica’s pore characteristics measured by gas adsorption. *Langmuir* 31:824–832
33. Zhou X, Wan QH (2015) Separation and identification of oligomeric phenylethoxysiloxanols by liquid chromatography–electrospray ionization mass spectrometry. *J Sep Sci* 38:1484–1490
34. Jiang Y, Wan QH (2015) Separation and identification of oligomeric ethyl silicates by liquid chromatography with electrospray ionization mass spectrometry. *J Chromatogr A* 1394:95–102
35. Jia G, Wan QH (2015) Separation and identification of oligomeric vinylmethoxysiloxanes by gradient elution chromatography coupled with electrospray ionization mass spectrometry. *J Chromatogr A* 1395:129–135
36. Zub YL, Stolyarchuk NV, Melnyk IV, Chuiko AA, Dabrowski A, Barczak M (2005) New adsorbents based on bridged polysilsesquioxanes containing 3-mercaptopropyl functional groups. *Mendeleeev Commun* 15:168–170
37. Nawrocki J (1997) The silanol group and its role in liquid chromatography. *J Chromatogr A* 779:29–71
38. Duchateau R, Dijkstra TW, van Santen RA, Yap GPA (2004) Silsesquioxane models for silica surface silanol sites with adjacent siloxide functionalites and olefin polymerization catalysts thereof. *Chem Eur J* 10:3979–3990
39. Chivers PT, Prehoda KE, Volkman BF, Kim BM, Markley JL, Raines RT (1997) Microscopic pK<sub>a</sub> values of *Escherichia coli* thioredoxin. *Biochemistry* 36:14985–14991
40. Poole CF (2015) An interphase model for retention in liquid chromatography. *J Planar Chromatogr* 28:98–105